AFWAL-TR-88-4165
ADA 204032

HYDROGEN-BONDED ION-ION INTERACTIONS IN A MOLTEN SALT PRECURSOR: THE CRYSTAL STRUCTURE OF 1-METHYL-3-ETHYLIMIDAZOLIUM CHLORIDE

C. J. Dymek, Jr.
The Frank J. Seiler Research Laboratory
United States Air Force Academy
Colorado Springs, Colorado 80840

David A. Grossie
Department of Chemistry
Wright State University
Dayton, Ohio 45435

Albert V. Fratini
Department of Chemistry
University of Dayton
Dayton, Ohio 45469

W. Wade Adams
Polymer Branch
Nonmetallic Materials Division

JUNE 1988

Interim Report for Period January 1987 - June 1988

MATERIALS LABORATORY
AIR FORCE WRIGHT AERONAUTICAL LABORATORIES
AIR FORCE SYSTEMS COMMAND
WRIGHT-PATTERSON AFB, OH 45433-6533

NOTICE

When Government drawings, specifications, or other data are used for any purpose other than in connection with a definitely Government-related procurement, the United States Government incurs no responsibility or any obligation whatsoever. The fact that the Government may have formulated or in any way supplied the said drawings, specifications, or other data, is not to be regarded by implication, or otherwise in any manner construed, as licensing the holder, or any other person or corporation; or as conveying any rights or permission to manufacture, use, or sell any patented invention that may in any way be related thereto.

This report has been reviewed by the Office of Public Affairs (ASD/PA) and is releasable to the National Technical Information Service (NTIS). At NTIS, it will be available to the general public including foreign nations.

This technical report has been reviewed and is approved for publication.

WALTER WADE ADAMS
Materials Research Engineer
Nonmetallic Materials Division

R. L. VAN DEUSEN, Chief
Polymer Branch
Nonmetallic Materials Division

FOR THE COMMANDER

MERRILL L. MINGES, Director
Nonmetallic Materials Division

If your address has changed, if you wish to be removed from our mailing list, or if the addressee is no longer employed by your organization, please notify AFWAL/MLBP, Wright-Patterson AFB, OH 45433-6533, to help us maintain a current mailing list.

Copies of this report should not be returned unless return is required by security considerations, contractual obligations, or notice on a specific document.

UNCLASSIFIED
SECURITY CLASSIFICATION OF THIS PAGE

REPORT DOCUMENTATION PAGE

Form Approved OMB No. 0704-0188

1a. REPORT SECURITY CLASSIFICATION: Unclassified	1b. RESTRICTIVE MARKINGS
2a. SECURITY CLASSIFICATION AUTHORITY	3. DISTRIBUTION/AVAILABILITY OF REPORT: Approved for Public Release, Distribution Unlimited.
2b. DECLASSIFICATION/DOWNGRADING SCHEDULE	
4. PERFORMING ORGANIZATION REPORT NUMBER(S): AFWAL-TR-88-4165	5. MONITORING ORGANIZATION REPORT NUMBER(S)
6a. NAME OF PERFORMING ORGANIZATION: Materials Laboratory; 6b. OFFICE SYMBOL (If applicable): AFWAL/MLBP	7a. NAME OF MONITORING ORGANIZATION
6c. ADDRESS (City, State, and ZIP Code): Wright-Patterson AFB, OH 45433-6533	7b. ADDRESS (City, State, and ZIP Code)
8a. NAME OF FUNDING/SPONSORING ORGANIZATION; 8b. OFFICE SYMBOL (If applicable)	9. PROCUREMENT INSTRUMENT IDENTIFICATION NUMBER
8c. ADDRESS (City, State, and ZIP Code)	10. SOURCE OF FUNDING NUMBERS

PROGRAM ELEMENT NO.	PROJECT NO.	TASK NO.	WORK UNIT ACCESSION NO.
61102F	2303	Q3	07

11. TITLE (Include Security Classification)
Hydrogen-Bonded Ion-Ion Interactions in a Molten Salt Precursor: The Crystal Structure of 1-Methyl-3-Ethylimidazolium Chloride

12. PERSONAL AUTHOR(S)
C. J. Dymek*, David A Grossie**, Albert V. Fratini***, and Walter Wade Adams

13a. TYPE OF REPORT	13b. TIME COVERED	14. DATE OF REPORT (Year, Month, Day)	15. PAGE COUNT
Interim	FROM Jan 87 TO Jun 88	1988 June	32

16. SUPPLEMENTARY NOTATION
*USAF Academy, **Wright State University, ***University of Dayton

17. COSATI CODES		
FIELD	GROUP	SUB-GROUP
07	04	
11	04	

18. SUBJECT TERMS (Continue on reverse if necessary and identify by block number)
Molten Salt; Electrolyte; Imidazolium Chloride; Hydrogen Bonding; Battery

19. ABSTRACT (Continue on reverse if necessary and identify by block number)
The crystal structure analysis of the molten salt precursor, 1-methyl-3-ethylimidazolium chloride (MEICl), was undertaken as part of an investigation of the ion-ion interactions in room temperature melts, where mole fraction N of $AlCl_3$ is less than 0.5. These melts are of interest as electrolytes in high energy density batteries, as solvents for studying ionic complexes, and as catalytic solvents for organic reactions. Hygroscopic crystals of MEICl were grown in acetonitrile and sealed under helium gas in a capillary tube. The orthorhombic space group is $P2_12_12_1$, with $\underline{a}$ = 10.087(1), $\underline{b}$ = 11.179(1), $\underline{c}$ = 28.733(4) Å, V = 3240.0 $Å^3$, mol. wt. = 146.62, D_{calc} = 1.204 g/cm^3 for Z = 16. The asymmetric unit contains four $MEI^+ \cdots Cl^-$ ion pairs. The MEI^+ ions cluster in four distinct layers perpendicular to the c-axis. Similarly, the arrangement of Cl^- ions is a layered one. Each Cl^- interacts with three MEI^+ ions and each MEI^+ is associated with three nearest Cl^- ions. The distance of Cl^- from a ring carbon atom averages 3.55 Å. Cl^- ions are situated in
(cont'd)

20. DISTRIBUTION/AVAILABILITY OF ABSTRACT	21. ABSTRACT SECURITY CLASSIFICATION
☒ UNCLASSIFIED/UNLIMITED ☐ SAME AS RPT. ☐ DTIC USERS	UNCLASSIFIED

22a. NAME OF RESPONSIBLE INDIVIDUAL	22b. TELEPHONE (Include Area Code)	22c. OFFICE SYMBOL
W. W. Adams	(513) 255-9148	AFWAL/MLBP

DD Form 1473, JUN 86 *Previous editions are obsolete.*

A. Abstract (continued)

potential hydrogen-bonded positions rather than at random, suggesting this interaction to be hydrogen bonding. Evidence for hydrogen bonding of Cl^- at the three ring C-H bonds in basic METCL/$AlCl_3$ melts is presented.

FOREWORD

This report was prepared by the Materials Laboratory Polymer Branch in collaboration with the Frank J. Seiler Research Laboratory, USAF Academy, the University of Dayton Chemistry Department, and the Wright State University Department of Chemistry. The work was initiated at the Frank J. Seiler Research Laboratory and performed at the Materials Laboratory under Project No. 2303, "Research to Define the Structure Property Relationships," Task No. 2303Q3 Work Unit Directive 2303Q307, "Structural Resins." Dr. Ivan J. Goldfarb served as the AFWAL/ML Work Unit Scientist. Co-authors were Lt. Col C. J. Dymek, Frank J. Seiler, Research Laboratory; Dr. D. A. Grossie, Wright State University; Dr. A. V. Fratini, University of Dayton; and Dr. W. W. Adams, Materials Laboratory (AFWAL/MLBP). Drs. D. A. Grossie and A. V. Fratini were supported by the Systran Corporation under Contract No. F33615-74-C-5116. This report covers research conducted from January 1987 to June 1988.

TABLE OF CONTENTS

LIST OF ILLUSTRATIONS

LIST OF TABLES

SECTION I

INTRODUCTION

Mixtures of 1-methyl-3-ethylimidazolium chloride, MEICl, and $AlCl_3$, where mole fraction, N, of $AlCl_3$ is between 0.33 and 0.67, are molten salts at and well below room temperature [1,2]. Pure MEICl has a melting point of 87°C. These melts are of interest as electrolytes in high energy-density batteries [3,4], as solvents for studying ionic complexes [5], and as catalytic solvents for organic reactions [6]. The potential utility of these melts has prompted studies into the nature of the ionic interactions in the melts.

IR spectroscopy [7] recently showed that the MEI^+ ion interacts with Cl^- ions present in basic melts (N < 0.5) at the C2, C4, and C5 positions shown in Figure 1. This result contrasts with the ion-pair model in which Cl^- is hydrogen bonded solely at the C2 position. An alternative model was suggested but not satisfactorily demonstrated in which the MEI^+ ions are stacked parallel to each other with Cl^- and $AlCl_4^-$ anions positioned such that Cl^- can interact with all three ring C-H bonds. Since the IR spectra of solid and liquid (90°C) MEICl were shown to be very similar, the x-ray crystal structure analysis of MEICl was undertaken to provide additional insight into the nature of $MEI^{+}\cdots Cl^-$ interactions in molten salts.

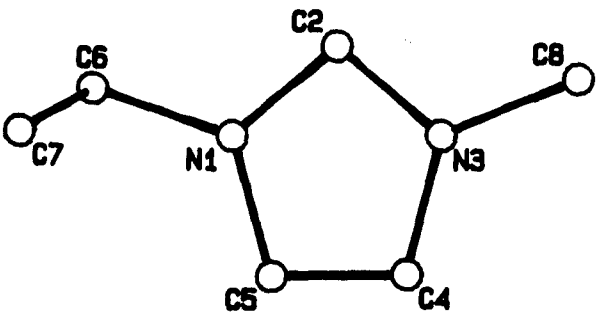

Figure 1. Structure of one of the four MEI^+ ions in the asymmetric unit.

SECTION II

EXPERIMENTAL METHODS

Solid MEICl was prepared in airless glassware as described previously [1] except that the solvent of recrystallization was acetonitrile rather than ethyl acetate, a procedure which enhanced crystal quality. About 3g of the crystals were placed under vacuum in a He-filled dry box and periodically weighed to monitor loss of any acetonitrile or unreacted reactants which might be adsorbed on or occluded in the crystals. After 5 days of pumping, the weight loss on overnight standing (15 hours) was only about 0.3 mg. The total weight loss over 9 days was 25 mg.

A small irregularly shaped crystal of MEICl was mounted in a glass capillary under dry box conditions. Preliminary examination and data collection were performed with MoKα radiation (λ = 0.71073 Å on an Enraf-Nonius CAD4 diffractometer equipped with a graphite crystal incident beam monochromator.

Cell constants and an orientation matrix for data collection were obtained from least-squares refinement, using the setting angles of 25 reflections in the range $5.0 < \theta < 16.3°$, measured by the computer controlled diagonal slit method of centering. The orthorhombic cell parameters and calculated volume are: $\underline{a}$ = 10.087(1), $\underline{b}$ = 11.179(1), $\underline{c}$ = 28.733(4) Å, V = 3240.0 Å^3. For Z = 16 and FW = 146.62, the calculated density is 1.20 g/cm^3, which compares with the measured density of 1.204 +/- 0.004 g/cm^3 obtained by flotation in a benzene/carbon tetrachloride mixture. Omega scans of

several intense reflections were measured at a take-off angle of 2.8°. The width at half-height was 0.85°, indicating poor crystal quality. From the observed systematic absences and subsequent least-squares refinement, the space group was determined to be $P2_12_12_1$ (# 19).

The data were collected at room temperature using the w-θ scan technique. The scan rate was calculated from the results of a fast pre-scan, and varied from 0.69 to 2.78°/min (in omega). Data were collected to a maximum 2θ of 50.0°. The scan range was determined as a function of θ to correct for the separation of the Kα doublet, and ranged from 0.9 to 1.1°. Horizontal and vertical aperture widths were set at 2.0 and 4.0 mm, respectively. The diameter of the incident beam collimator was 0.4 mm and the crystal-to-detector distance was 21 cm. For intense reflections a zirconium foil with an attenuation factor of 12.06 was automatically inserted in front of the detector.

Three representative reflections were measured every 30 min as a check on crystal and electronic stability. The intensities of these standards remained constant within experimental error throughout data collection. Despite the extreme hygroscopic nature of the compound, the crystal remained intact throughout the data collection and no decay correction was applied. We collected 3284 unique reflections. Lorentz and polarization corrections were applied to the data. The linear absorption coefficient is 3.9 cm^{-1} for MoKα radiation and no absorption correction was made.

The structure was solved by direct methods [9]. All non-hydrogen atoms were located in an E-map prepared from the phase set with the highest confined figure of merit. Hydrogen atoms were located and added to the structure factor calculations but their positions were not refined. The structure was refined by full matrix least-squares [10] where the function minimized was $\Sigma w(|Fo|-|Fc|)^2$ and the weight w is defined as the reciprocal of the standard deviation on Fo, squared. Atomic scattering factors were taken from Cromer and Waber [11] and the values for $\Delta f'$ and $\Delta f''$ were those of Cromer [11].

Eight hundred and sixty five reflections having intensities greater than 3.0 times their standard deviation were used in the refinements. The final cycle of refinement included 159 variable parameters and converged (largest parameter shift was 0.07 times its estimated standard deviation) with unweighted and weighted agreement factors of 0.10 and 0.13, respectively. The standard deviation of an observation of unit weight was 3.63. The highest peak in the final difference Fourier map had a height of 0.44 e/Å^3 with an estimated error based on ΔF of 0.10, while the largest negative peak had a height of 0.41 e/Å^3.

Fractional coordinates and equivalent isotropic thermal parameters for the 36 nonhydrogen atoms are reported in Table 1.

Table 1

Fractional Coordinates and Equivalent Isotropic Thermal Parameters and Their Estimated Standard Deviations

	Atom	x	y	z	B(Å²)*
MEI⁺(1)	N1	0.834(3)	0.673(2)	0.5846(8)	6.3(7)
	C2	0.758(3)	0.742(3)	0.562(1)	7(1)
	N3	0.680(2)	0.800(2)	0.5907(7)	4.8(6)
	C4	0.701(3)	0.765(2)	0.6355(8)	3.4(6)
	C5	0.804(3)	0.680(3)	0.6325(9)	5.6(8)
	C6	0.944(3)	0.599(3)	0.568(1)	8(1)
	C7	0.913(4)	0.478(4)	0.568(1)	15(2)
	C8	0.581(3)	0.883(3)	0.577(1)	6.3(9)
MEI⁺(2)	N11	-0.065(2)	0.014(2)	0.4069(8)	5.5(7)
	C12	-0.118(3)	-0.054(3)	0.3799(9)	5.3(8)
	N13	-0.072(2)	-0.050(2)	0.3393(7)	5.0(6)
	C14	0.019(3)	0.047(3)	0.334(1)	6.4(9)
	C15	0.044(4)	0.078(3)	0.381(1)	9(1)
	C16	-0.090(3)	0.052(3)	0.460(1)	6.8(9)
	C17	0.008(4)	-0.032(3)	0.481(1)	11(1)
	C18	-0.129(3)	-0.121(3)	0.2984(9)	6.1(9)
MEI⁺(3)	N21	0.752(3)	0.289(3)	0.341(1)	9.4(9)
	C22	0.813(3)	0.366(3)	0.3668(9)	6.0(9)
	N23	0.783(2)	0.340(2)	0.4104(7)	4.1(6)
	C24	0.685(3)	0.250(3)	0.4096(9)	4.8(8)

	C25	0.671(4)	0.217(3)	0.364(1)	9(1)
	C26	0.807 [b]	0.250 [b]	0.285 [b]	12(1)
	C27	0.723 [b]	0.279 [b]	0.262 [b]	16(2)
	C28	0.822(3)	0.398(2)	0.4538(9)	5.0(8)
$MEI^+(4)$	N31	0.642(2)	-0.060(2)	0.1583(7)	4.0(5)
	C32	0.565(2)	-0.001(2)	0.1866(8)	3.0(6)
	N33	0.482(2)	0.063(2)	0.1623(7)	3.7(5)
	C34	0.495(3)	0.043(3)	0.1169(9)	4.4(7)
	C35	0.589(3)	-0.039(3)	0.115(1)	5.0(8)
	C36	0.764(3)	-0.145(3)	0.167(1)	7(1)
	C37	0.714(3)	-0.232(3)	0.197(1)	8(1)
	C38	0.390(3)	0.154(3)	0.184(1)	7(1)
	CL1	0.2339(9)	0.7793(8)	0.5556(3)	5.8(2) *
	CL2	0.476(1)	0.9408(8)	0.7042(3)	6.6(2) *
	CL3	-0.173(1)	0.8055(8)	1.0402(3)	6.6(2) *
	CL4	-0.466(1)	0.9774(8)	1.3019(3)	6.4(2) *

[a] An asterisk indicates that the atoms were refined anisotropically and are given in the form of the isotropic equivalent thermal parameter defined as: $(4/3)[a^2B_{11} + b^2B_{22} + c^2B_{33} + ab(\cos\gamma)B_{12} + ac(\cos\beta)B_{13} + bc(\cos\alpha)B_{23}]$.

[b] Parameter was fixed during the final cycle of least-squares refinement.

SECTION III

DISCUSSION

A. MEI^+ Cation

The asymmetric unit consists of four $MEI^+\cdots Cl^-$ ion pairs. Figure 1 shows a view of one of the four substituted imidazolium ions. The endocyclic bond distances and angles in the four MEI^+ ions vary markedly from ring to ring (1.21-1.51 Å and 101-114°). The exocyclic alkyl groups are attached to the ring with bond distances of 1.43-1.74 Å. In $MEI^+(2)$ and $MEI^+(4)$ ions, the beta carbon of each ethyl substituent is above the mean plane of the five-membered ring, with torsion angles (C12-N11-C16-C17 and C32-N31-C36-C37) of 96.3 and 55.7°, respectively, while in the $MEI^+(1)$, the beta carbon is below the ring, with a torsion angle (C2-N1-C6-C7) of -107.3°. The ethyl substituent of the fourth cation ($MEI^+(3)$) is disordered. This observation simply reflects the poor crystal quality of these molten salts precursors. Table 2 summarizes the pertinent bond distances and angles and dihedral angles.

B. Unit Cell

As shown in Figure 2, the ion pairs pack into the unit cell in ways similar to both planar molecules and simple inorganic salts. The MEI^+ ions cluster in four distinct layers, perpendicular to the c-axis, with interlayer separations of 6.741-7.568 Å as defined by the average distances between ring centroids. Each of these layers has one of two possible repeating patterns. The first pattern, found at about z = 0.13 and 0.87, consists of groups of three ions with their ring

Table 2

Bond Distances

Bond	MEI(1)	MEI(2)	MEI(3)	MEI(4)	Average
N1-C2	1.27(5)	1.21(4)	1.29(4)	1.30(3)	1.27
C2-N3	1.32(4)	1.25(3)	1.33(3)	1.31(3)	1.30
N3-C4	1.36(3)	1.43(4)	1.41(4)	1.34(3)	1.39
C4-C5	1.42(4)	1.42(4)	1.36(4)	1.32(4)	1.38
C5-N1	1.42(4)	1.51(4)	1.33(5)	1.38(3)	1.41
N1-C6	1.46(4)	1.61(4)	1.74(3)*	1.57(4)	1.55
C6-C7	1.39(5)	1.49(5)	1.14(4)*	1.40(4)	1.43
N3-C8	1.43(4)	1.53(4)	1.46(4)	1.51(4)	1.48

Bond Angles

Angle	MEI(1)	MEI(2)	MEI(3)	MEI(4)	Average
C2-N1-C5	110(3)	107(2)	113(3)	105(2)	109
N1-C2-N3	109(3)	114(3)	107(3)	109(3)	110
C2-N3-C4	112(2)	113(2)	107(2)	112(2)	111
N3-C4-C5	105(2)	105(2)	101(2)	106(3)	104
C4-C5-N1	105(2)	103(3)	105(4)	110(2)	106
C2-N1-C6	129(3)	135(2)	123(2)	132(3)	130
C5-N1-C6	121(2)	118(2)	120(2)	123(2)	121
C2-N3-C8	124(2)	124(2)	132(2)	123(3)	126
C4-N3-C8	124(2)	123(2)	121(3)	125(2)	123
N1-C6-C7	112(4)	96(2)	104(1)	104(3)	104

Dihedral Angles

Angle	MEI(1)	MEI(2)	MEI(3)	MEI(4)
C2-N1-C6-C7	-107(4)	96(4)	-118(3)	56(4)

* Omitted from the average bond distance.

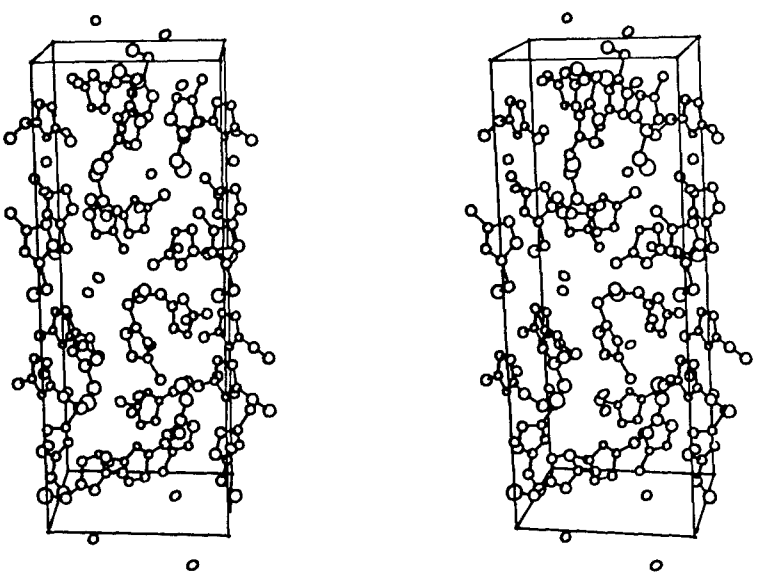

Figure 2. Stereoview of the MEICl unit cell. The c-axis is vertical and a is horizontal.

normals positioned midway between and parallel to ab cell diagonals. Within a layer, each molecule is separated from its neighbor by 3.792-4.091 Å measured along the diagonal, while the edge-to-edge separation is 7.381-7.704 Å. The layer at z = 0.87 is rotated 90° from the z = 0.13 layer.

The second pattern is found at z = 0.37 and 0.64 and is composed of rows of five cations separated from neighboring rows by 7.381-7.704 Å. The middle layers differ in orientation in the same manner as do the first and last layers.

The Cl^- ions are arrayed throughout the unit cell as shown in Figure 3. As described for the MEI^+ ions, the arrangement is a layered one, comprising four different patterns of anions. The first two patterns at z = -0.05 and 0.05 are related by space group symmetry, each consisting of a pair of Cl^- ions situated approximately on ab cell diagonals. The third and fourth patterns are found at z = 0.30 and 0.70, the former consisting of four ions located approximately on the ac and bc faces of the unit cell, while the latter is comprised of a plane of five ions, one close to each cell edge and the fifth approximately in the center of the cell. These four patterns occur cyclically along the c-axis, the first occurrence of the first and second patterns being split by the bottom ab face of the unit cell. The fourth pattern occurs after this, followed by the third. In the center of the cell, the first and second patterns repeat, after which the third and fourth patterns repeat, and so on.

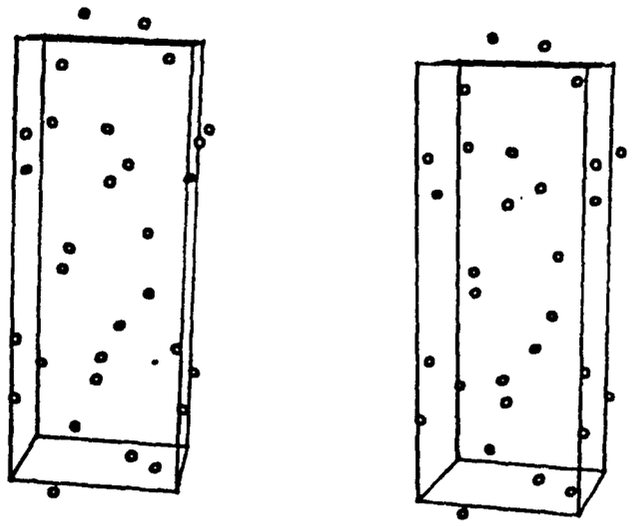

Figure 3. Stereoview of the arrangement of Cl^- ions in the unit cell. The c-axis is vertical and a is horizontal.

C. Interlayer Interactions

The layered structure evident in the unit cell can be extrapolated to characterize the overall structure of the MEICl crystal. The layers of Cl^- ions lie between the MEI^+ layers to form the complete structure as shown schematically in Figure 4. In this figure, the large circles and lines represent the MEI^+ ions and the smaller circles the Cl^- ions. Thicker lines and larger circles (closer to the viewer) are used to suggest the perspective. The direction of the stacks in a layer is rotated 90° from the direction of adjacent layers.

The relative orientations and connectivity of the layers are suggested by the drawing in Figure 5. In this drawing, the cations are shown arranged in rows (designated a through h) in which the MEI^+ rings share a common plane (see the corresponding row enclosed in the dashed rectangle in Figure 4). The rows in the plane of the drawing (a, c, e, and g) represent a cross section of the layers formed by the staggered stacks of MEI^+ running parallel to the plane of the drawing. The alternating rows running perpendicular to the plane of the drawing (b, d, f, and h) represent a similar cross section. The heavy dashed line (the c-axis of the unit cell) is at the intersection of these two cross sections. Note that the rows labelled a and e are equivalent. The light dashed lines connect Cl^- and MEI^+ ions which are nearest neighbors. By examining the Cl^- ions on the intersection line, we can see that each Cl^- interacts with three MEI^+ ions, two of

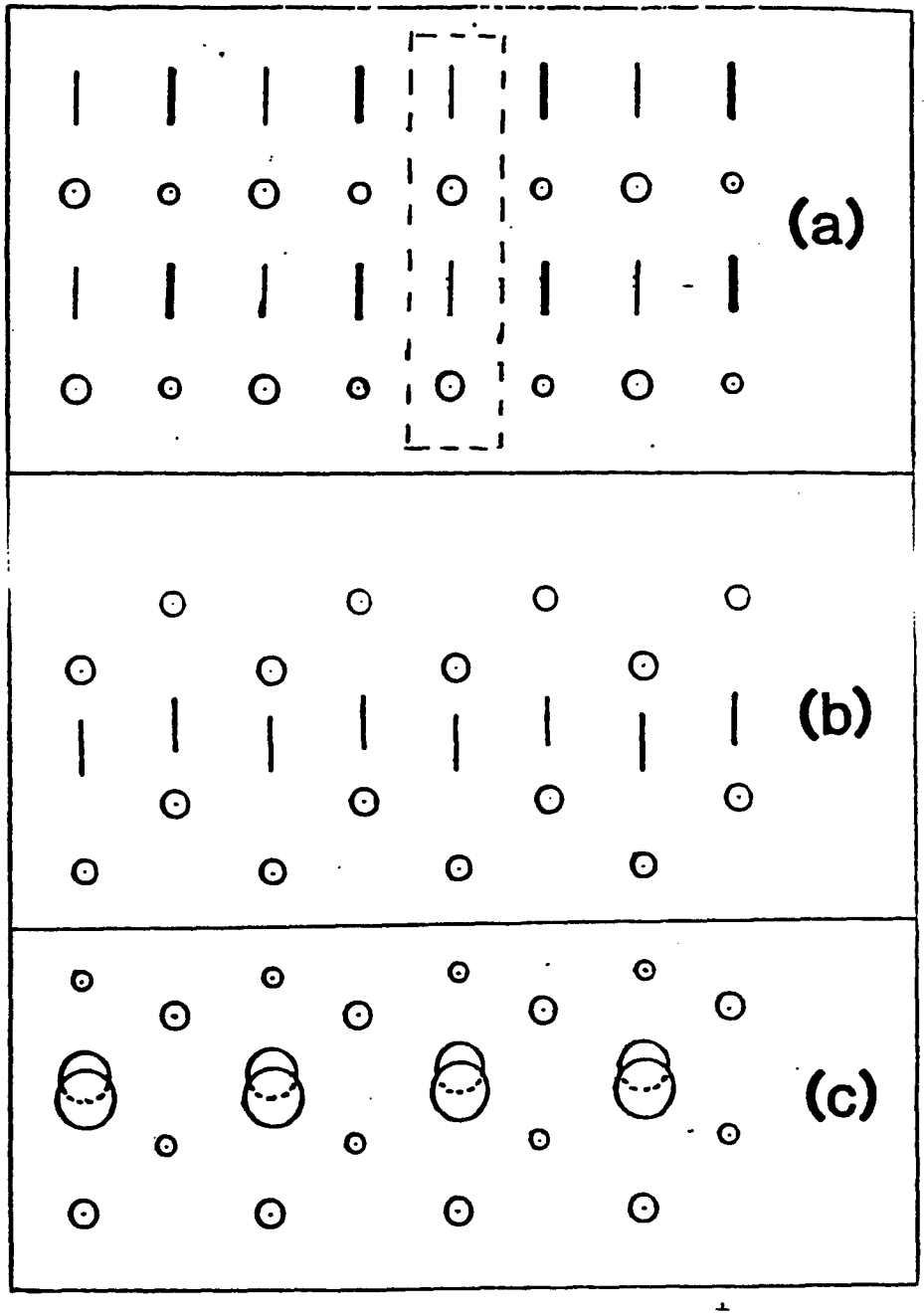

Figure 4. Schematic representation of layers of MEI^+ stacks with adjacent Cl^- ions. (a) Top view, (b)(c) Side views. Large circles and lines represent MEI^+ ions and the smaller circles the Cl^- ions. The dashed rectangle in (a) encloses a row of MEI^+ rings which share a common plane.

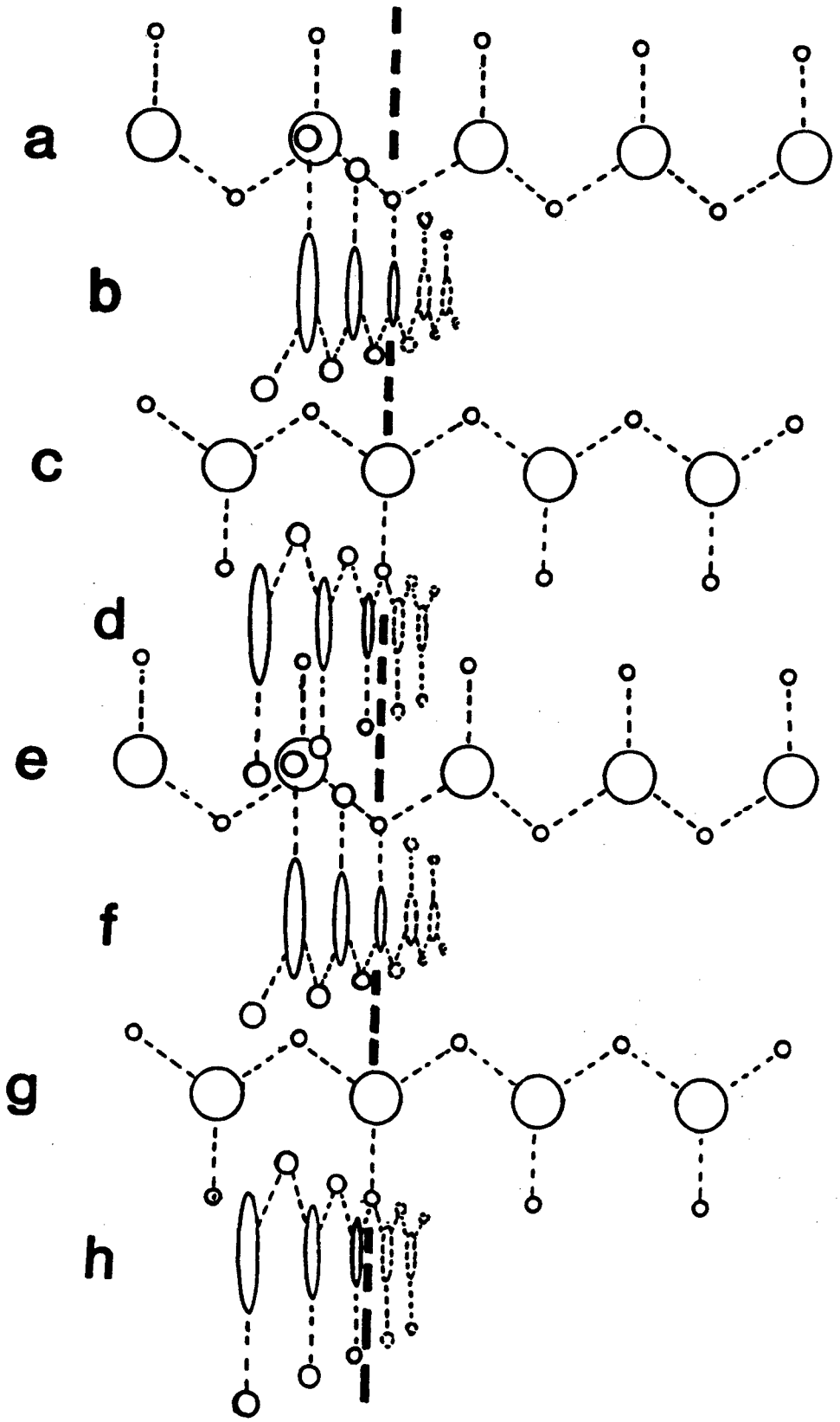

Figure 5. Overall MEICl structure showing relative orientation and connectivity of adjacent layers. Rows a and e are equivalent. Heavy dashed line represents the direction of the c-axis.

which share a plane which is perpendicular to the plane of the third. Also, each MEI^+ is associated with three nearest Cl^- ions which are in the same plane as the MEI^+ ring.

There are two rows of Cl^- ions associated with each row of MEI^+ ions. One has Cl^- ions interacting with just a single ring carbon atom (alternating between C2 and C5) of the MEI^+ ion in an associated row, while another (on the side of the MEI^+ row) has each Cl^- interacting with ring carbon atoms from two adjacent MEI^+ ions in the row. In Figure 5 these would be the top and bottom Cl^- rows, respectively, interacting with row (a) of MEI^+ ions. These rows are drawn with uniformly spaced Cl^- ions; however, in the crystal the spacings are alternately large and small. In the top row, the Cl^- ions interacting with C2 are directly above the MEI^+, while those interacting with C5 are forced to shift in the direction of the C5-H bond and as a consequence away from positions directly above the MEI^+. If the interaction of Cl^- with MEI^+ were non-specific, the Cl^- ions would be expected to be uniformly spaced to achieve maximum separation. This uneven spacing is seen as evidence for Cl^- ions interacting specifically with MEI^+ through hydrogen bonding.

D. Ion-Ion Interactions

Figure 5 shows that the stack model in which Cl^- ions are positioned between stacked MEI^+ ions is not supported by the crystal structure and that the C2-H$\cdots$$Cl^-$ hydrogen-bonded ion-pair model is preferred. The dominant feature of the triple interactions of each ion in the structure is illustrated

in Figure 6. These figures were abstracted from the stereoscopic view shown in Figure 2. The distance of a Cl^- from a ring carbon atom averages about 3.55 Å, ranging from 3.34 to 3.80 Å. This is in good agreement with the accepted criteria for C-H···Cl^- hydrogen bonding [8]. However, the fact that the Cl^- ions are situated in potential hydrogen-bonded positions (C-H···Cl^- angle ranges from 132 to 167°) rather than at random strongly suggests this interaction to be hydrogen bonding. Further evidence for a hydrogen-bonded interaction is provided by ring C-H stretching bands which shift to lower frequencies (by about 100-150 cm^{-1}) and become broader and more intense as more Cl^- is present in basic MEICl/$AlCl_3$ melts [7]. Thus, the C2-H···Cl^- hydrogen-bonded ion pair model should account for C-H···Cl^- type interaction at all three ring carbon atoms.

E. Arrangement of Alkyl Substutuents in Stacks

In the stacks of MEI^+ ions, the ethyl and methyl groups are arranged in a pattern which is shown by the stack of 5 MEI^+ ions at z = 0.65 going from the left rear to the right front (Figure 2). Starting with the right front MEI^+ and going back, the direction of the ethyl groups from the ring center is

Down - Right - Left - Up - Down

└──────────────────────────┘

equivalent

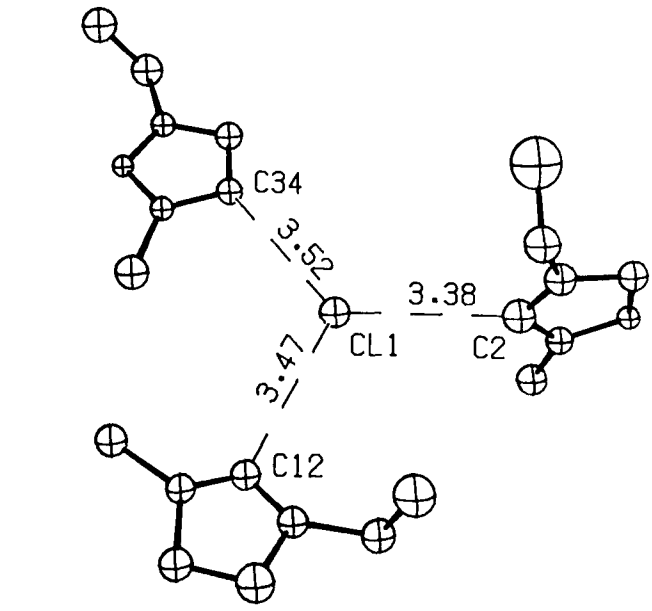

(a)

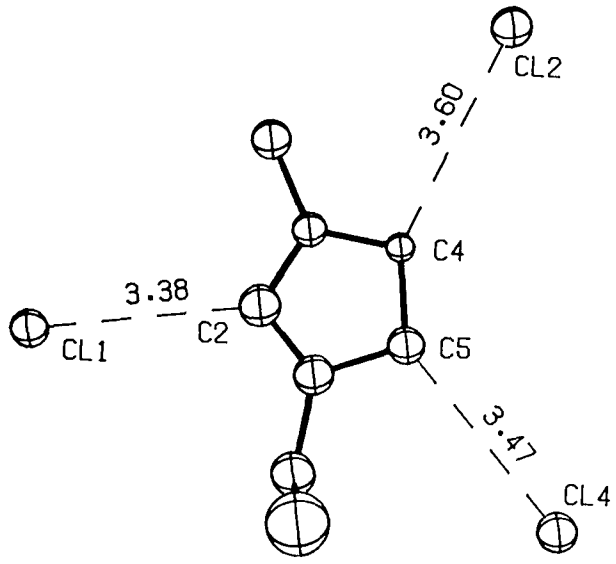

(b)

Figure 6. Abstracted views from Fig. 2 showing (a) interaction of Cl^- with three nearest MEI^+ ions, (b) interaction of MEI^+ with three nearest Cl^- ions.

If we go to the stack just below it at z = 0.35 that runs from left front to rear right, the order of the direction of the ethyl groups is

Right - Down - Up - Left - Right

equivalent

This second order can be visualized as resulting from rotating through 180° around the axis of the stack first described. Another way of describing the ring orientation is to give the order of rotations around the stack axis that successive MEI^+ ions undergo. The sequence of rotations is: -90°, 180°, 90°, 180°, -90°, 180°, 90°, 180°, -90°, etc. Any sequence of MEI^+'s stacked in the unit cell follow this order of relative orientations.

F. Arrangement of Alkyl Substituents in Rows

The rows of MEI^+ ions in which they share the same plane (as shown in Figure 5) have a simpler sequence of relative orientations. It is: 90°, -90°, 90°, -90°, etc. Thus each MEI^+ in a row is rotated 90° from its two adjacent MEI^+ ions, and every other MEI^+ ion (or alternating MEI^+'s) have exactly the same orientation.

G. Extension of Model to Liquid Phase

The shift in frequency and broadening of the MEI^+ ring C-H stretching band observed in basic $MEICl/AlCl_3$ melts [7] is certainly consistent with the aforementioned hydrogen-bonding

model. An equally compelling observation is the comparison of the IR spectra of solid and liquid MEICl shown in Figure 7. This previously presented [12] but unpublished result supports the conclusions that the interactions with Cl^- affecting the ring C-H stretches in MEI^+ are virtually the same in the solid and liquid phases of MEICl. The presence of $AlCl_4^-$ in basic melts may alter the $MEI^+\cdots Cl^-$ interaction only slightly since the peaks of the ring C-H stretching bands in liquid MEICl and basic MEICl/$AlCl_3$ melts are also virtually the same ("the Cl^- interaction band"is at 3049 cm^{-1} [7]). Thus the $MEI^+\cdots Cl^-$ interactions in basic melts are characterized as hydrogen-bonding of Cl^- at the three ring C-H bonds.

H. Conclusions

The structure of crystalline MEICl is characterized by layers containing MEI^+ ions interspersed with layers of Cl^- ions. The directions of the stacks in adjacent layers are rotated 90°. Each MEI^+ ion appears to be hydrogen bonded to three nearest Cl^- ions. The results suggest that in basic MEICl/$AlCl_3$ molten salts, the Cl^- ions also interact with MEI^+ by hydrogen bonding at the three ring carbon atoms.

See Appendix A for listing of anisotropic thermal parameters for Cl^- (1 page); see Appendix B for a listing of observed and calculated structure factor amplitudes (5 pages).

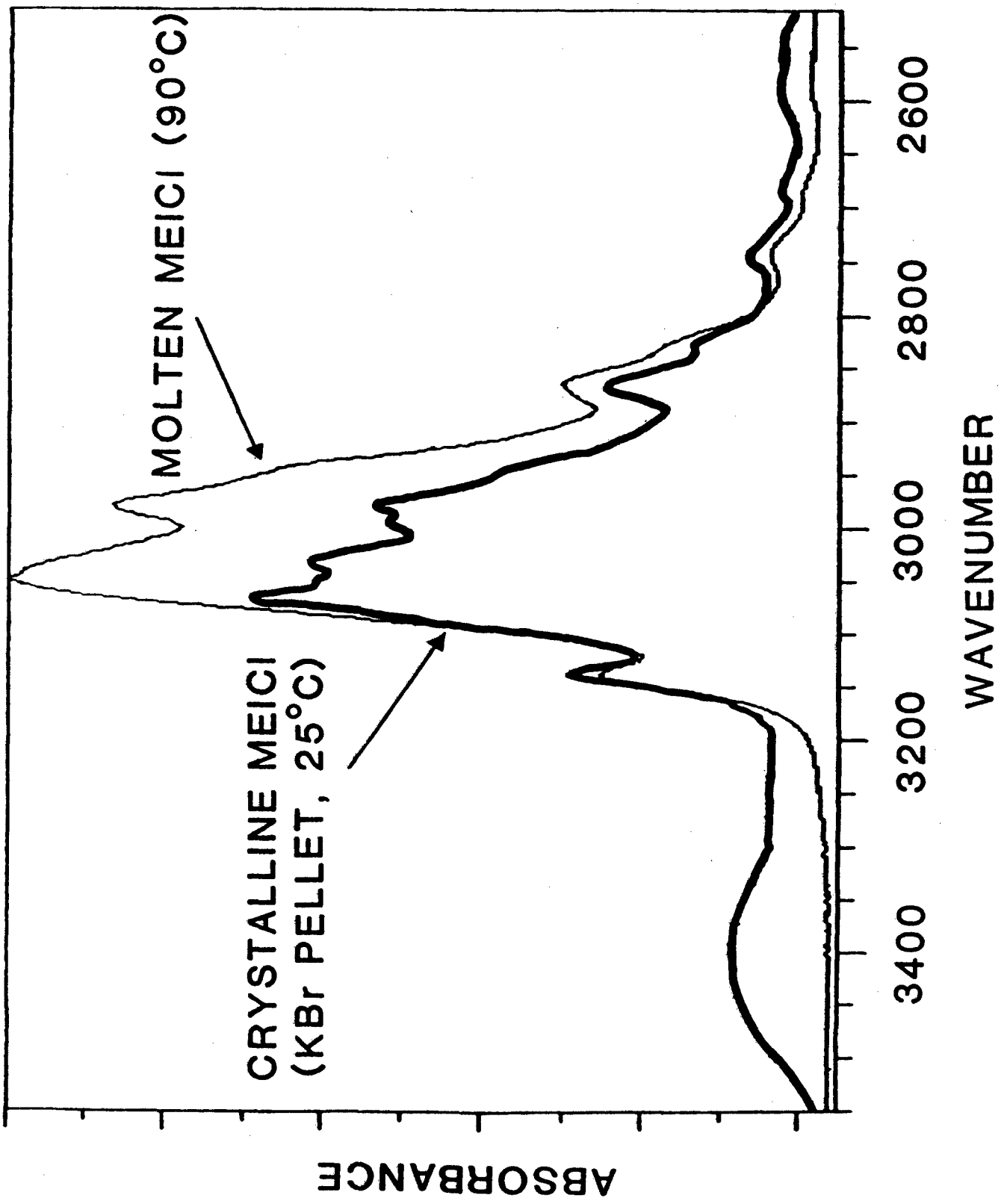

Figure 7. FTIR spectra of solid and liquid MEICl. Liquid MEICl sample was a thin film between NaCl plates with no spacers. Spectra recorded on an IBM IR/32 FTIR spectrometer [12].

REFERENCES

1. Wilkes, J. S.; Levisky, J. A.; Wilson, R. A.; Hussey, C. L.; Inorg. Chem., 21, 1263 (1982).

2. Fannin, A. A., Jr.; Floreani, D. A.; King, L. A.; Landers, J. S.; Piersma, B. J.; Stech, D. J.; Vaughn, R. L.; Wilkes, J. S.; Williams, J. L.; J. Phys. Chem, 88, (1984).

3. Reynolds, G. F.; Dymek, C. J., Jr.; J. Power Sources, 15, 109 (1985).

4. Dymek, C. J., Jr.; Reynolds, G. F.; Wilkes, J. S.; J. Electrochem. Soc., 134 (7), 1658 (1987).

5. Hussey, C. L., Adv. Molten Salt Chem., G. Mantov and C. Mamantov, ed., Elsevier, New York, 15, 185 (1983).

6. Boon, J. A.; Levisky, J. A.; Pflug, J. L.; and Wilkes, J. S.; J. Org. Chem., 51, 480 (1986).

7. Dieter, K. M.; Dymek, C. J., Jr.; Heimer, N. E.; Rovang, J. W.; and Wilkes, J. S.; "Ionic Structure and Interactions in 1-Methyl-3-Ethylimidazolium Chloride/$AlCl_3$ Molten Salts," Proc. Of the Joint International Symposium on Molten Salts, 172nd Meeting of the Electrochemical Society, Honolulu, HI, Oct 87.

8. Taylor, R. and Kennard, O., J. Am. Chem. Soc., 104, 5063 (1982).

9. Main, P. (1982). Editor, MULTAN 11/82. A System of Computer Programs for the Automatic Solution of Crystal Structures from X-ray Diffraction Data. Univ. of York, England. 2. Enraf-Nonius (1982). SDP/VAX. A System of Programs for Crystal Structure Determination. 10. Enraf-Nonius (1982). SDP/VAX. A System of Programs for Crystal Structure Determination.

11. International Tables for X-ray Crystallography (1974). Vol. IV, Birmingham: Kynoch Press.

12. Dieter, K.M., Dymek, C.J., Jr., Heimer, N.E., Rovang, J.W., and Wilkes, J.S., "Ionic Structure and Interactions in 1-Methyl-3-ethylimidazolium Chloride/$AlCl_3$ Molten Salts," 172nd Meeting of the Electrochemical Society, Honolulu, HI, Oct. 1987.

Appendix A

Table of General Displacement Parameter Expressions - U's

Name	U(1,1)	U(2,2)	U(3,3)	U(1,2)	U(1,3)	U(2,3)
CL1	0.087(7)	0.071(6)	0.062(5)	0.013(6)	0.008(5)	0.002(5)
CL2	0.105(7)	0.076(6)	0.072(5)	-0.022(6)	-0.012(6)	0.000(6)
CL3	0.100(7)	0.086(7)	0.064(5)	0.013(7)	0.002(6)	-0.014(6)
CL4	0.105(7)	0.089(6)	0.048(5)	-0.017(7)	0.017(5)	-0.014(5)

Appendix B

Observed and Calculated Structure Factor Amplitudes

Values of 10*Fobs and 10*Fcalc

H	K	L	Fobs	Fcalc	SigF	H	K	L	Fobs	Fcalc	SigF	H	K	L	Fobs	Fcalc	SigF	H	K	L	Fobs	Fcalc	SigF
0	0	2	96	105	3	0	3	7	489	553	10	0	6	18	303	299	11	1	1	4	498	388	6
0	0	4	1605	1679	4	0	3	8	421	421	11	0	6	22	189	156	17	1	1	5	764	734	6
0	0	8	2119	2133	6	0	3	9	521	648	10	0	6	25	161	202	21	1	1	6	540	497	7
0	0	10	110	58	15	0	3	10	332	253	13	0	7	2	312	344	15	1	1	7	2270	2192	6
0	0	12	906	893	8	0	3	11	456	439	11	0	7	3	415	427	15	1	1	8	503	442	9
0	0	16	160	86	13	0	3	13	182	163	11	0	7	6	171	502	15	1	1	10	166	142	10
0	0	20	547	545	13	0	3	16	124	170	18	0	7	11	219	205	13	1	1	11	264	273	11
0	0	22	156	105	18	0	3	17	543	488	13	0	7	12	134	113	20	1	1	13	316	337	11
0	0	24	457	413	17	0	3	18	341	323	13	0	7	14	178	166	17	1	1	14	264	258	10
0	0	28	427	369	16	0	3	20	192	241	15	0	7	15	213	187	15	1	1	15	1220	1190	9
0	1	1	189	186	6	0	3	21	164	139	18	0	7	18	416	349	13	1	1	16	307	316	10
0	1	2	188	176	7	0	3	25	321	325	14	0	8	0	289	283	11	1	1	17	637	627	11
0	1	3	170	100	6	0	3	26	218	174	15	0	8	1	224	205	13	1	1	20	132	107	19
0	1	4	479	448	6	0	3	29	147	63	20	0	8	10	147	147	20	1	1	21	334	359	12
0	1	5	480	435	6	0	3	33	159	53	22	0	8	13	145	86	21	1	1	29	176	165	18
0	1	7	705	767	7	0	4	0	1337	1303	7	0	8	16	195	210	16	1	2	0	341	344	8
0	1	8	213	224	8	0	4	1	441	416	10	0	8	24	186	155	19	1	2	1	277	259	9
0	1	9	268	187	12	0	4	4	109	89	15	0	9	12	163	149	19	1	2	2	150	134	7
0	1	11	343	294	12	0	4	8	281	375	9	0	9	13	230	202	14	1	2	3	180	208	7
0	1	12	216	211	9	0	4	11	286	294	10	0	9	16	185	141	17	1	2	5	299	365	10
0	1	15	779	829	10	0	4	12	272	353	12	0	10	2	200	175	16	1	2	6	598	538	8
0	1	16	336	295	12	0	4	15	194	154	13	0	10	3	291	287	17	1	2	7	218	177	8
0	1	17	319	270	13	0	4	16	147	167	17	0	10	11	193	165	17	1	2	8	299	319	12
0	1	23	147	225	21	0	4	17	192	214	14	1	0	2	155	144	7	1	2	9	625	587	8
0	1	25	251	201	14	0	4	19	224	216	13	1	0	3	355	307	6	1	2	10	570	591	9
0	2	0	203	262	9	0	4	20	297	308	13	1	0	4	429	337	6	1	2	11	233	260	9
0	2	1	509	472	6	0	4	21	202	228	16	1	0	5	661	641	6	1	2	12	378	385	12
0	2	2	973	942	5	0	4	23	282	275	12	1	0	6	468	373	7	1	2	13	158	147	12
0	2	3	416	446	7	0	4	28	153	153	21	1	0	7	128	131	10	1	2	14	340	316	13
0	2	4	181	177	8	0	5	1	336	329	12	1	0	8	395	340	10	1	2	15	312	292	11
0	2	6	1058	984	7	0	5	3	191	176	10	1	0	9	531	578	9	1	2	17	163	158	14
0	2	7	220	220	9	0	5	4	377	475	8	1	0	10	141	119	12	1	2	18	173	234	15
0	2	9	563	525	9	0	5	11	212	209	11	1	0	11	385	420	12	1	2	20	308	308	11
0	2	10	1277	1158	8	0	5	13	238	244	12	1	0	12	234	197	9	1	2	22	222	231	14
0	2	13	130	135	14	0	5	15	341	320	13	1	0	14	223	230	9	1	2	25	230	179	14
0	2	14	222	175	9	0	5	16	451	425	15	1	0	15	280	276	9	1	2	32	159	138	22
0	2	19	205	202	13	0	5	27	152	164	22	1	0	17	328	379	13	1	3	0	743	648	7
0	2	22	555	614	15	0	6	0	212	186	10	1	0	20	200	201	13	1	3	1	1357	1368	7
0	2	26	266	265	13	0	6	1	187	166	12	1	0	22	264	282	12	1	3	2	231	230	10
0	3	2	1165	1117	6	0	6	3	279	252	11	1	0	25	206	240	17	1	3	3	388	348	11
0	3	3	1108	1010	7	0	6	10	310	341	10	1	1	0	301	330	6	1	3	4	472	542	10
0	3	4	650	680	8	0	6	12	141	129	18	1	1	1	796	663	4	1	3	5	1515	1424	7
0	3	5	751	1173	8	0	6	13	222	236	12	1	1	2	341	409	6	1	3	6	487	472	10
0	3	6	917	933	8	0	6	14	209	225	14	1	1	3	758	812	5	1	3	7	998	923	8

Values of 10*Fobs and 10*Fcalc

H	K	L	Fobs	Fcalc	SigF	H	K	L	Fobs	Fcalc	SigF	H	K	L	Fobs	Fcalc	SigF	H	K	L	Fobs	Fcalc	SigF
1	3	8	201	213	9	1	5	21	145	136	20	2	0	5	125	94	10	2	2	13	136	148	14
1	3	9	258	256	10	1	5	22	184	154	17	2	0	6	827	774	7	2	2	14	158	130	13
1	3	10	185	192	10	1	5	25	145	144	20	2	0	9	266	270	11	2	2	15	337	312	14
1	3	11	117	92	16	1	6	0	292	277	11	2	0	10	1434	1386	8	2	2	17	174	165	14
1	3	12	200	220	10	1	6	1	664	634	11	2	0	13	147	186	12	2	2	19	157	157	16
1	3	13	408	387	12	1	6	2	509	501	12	2	0	18	140	168	17	2	2	20	413	375	16
1	3	14	129	163	16	1	6	3	497	464	12	2	0	19	195	149	13	2	2	23	268	252	12
1	3	15	765	738	11	1	6	4	195	236	12	2	0	21	172	208	16	2	2	24	161	125	19
1	3	16	230	270	11	1	6	8	187	268	13	2	0	22	528	599	15	2	2	28	228	233	15
1	3	17	238	196	11	1	6	9	167	352	15	2	0	26	226	240	14	2	3	0	362	340	11
1	3	18	158	165	16	1	6	10	458	448	14	2	1	0	122	91	9	2	3	1	1161	1056	7
1	3	20	192	163	15	1	6	11	599	544	13	2	1	1	255	240	10	2	3	2	678	715	8
1	3	23	298	272	11	1	6	12	206	211	13	2	1	2	821	701	6	2	3	3	216	151	8
1	3	30	158	90	20	1	6	13	345	332	16	2	1	3	1158	1123	6	2	3	4	325	316	12
1	4	0	735	698	8	1	6	15	172	137	16	2	1	4	497	485	8	2	3	5	251	211	10
1	4	1	844	758	8	1	6	16	177	151	16	2	1	5	1110	1021	7	2	3	6	214	161	10
1	4	2	336	353	12	1	6	17	216	212	14	2	1	6	408	383	10	2	3	7	744	659	9
1	4	3	396	346	11	1	6	18	228	220	14	2	1	8	473	446	9	2	3	8	203	231	9
1	4	4	382	358	11	1	6	20	165	201	19	2	1	9	293	241	10	2	3	9	465	487	11
1	4	7	181	219	10	1	6	21	144	127	20	2	1	10	196	249	10	2	3	10	356	318	11
1	4	8	525	573	10	1	7	2	154	139	16	2	1	11	431	406	11	2	3	11	297	263	11
1	4	9	515	527	11	1	7	6	146	87	16	2	1	12	279	220	10	2	3	12	142	152	14
1	4	10	403	389	12	1	7	7	192	307	15	2	1	13	178	166	11	2	3	14	163	196	13
1	4	11	658	602	11	1	7	16	157	158	19	2	1	14	164	149	12	2	3	15	460	457	13
1	4	12	609	553	11	1	7	17	158	99	19	2	1	15	374	347	13	2	3	16	352	349	13
1	4	13	517	473	12	1	7	18	170	178	19	2	1	17	452	434	14	2	3	19	279	288	16
1	4	14	164	162	14	1	7	23	148	83	20	2	1	18	141	117	16	2	3	27	225	209	14
1	4	15	286	236	9	1	7	24	152	99	20	2	1	21	156	183	18	2	4	1	353	273	11
1	4	17	339	295	13	1	8	1	265	222	12	2	1	22	143	102	19	2	4	2	452	440	10
1	4	18	228	208	12	1	8	3	179	205	16	2	1	25	323	277	11	2	4	6	431	434	11
1	4	20	275	292	13	1	8	7	155	274	19	2	1	26	172	121	18	2	4	8	590	578	10
1	5	0	121	75	15	1	8	11	275	251	12	2	2	0	3779	4142	6	2	4	9	164	173	12
1	5	1	251	200	9	1	8	13	141	116	21	2	2	1	1650	1669	6	2	4	10	589	601	11
1	5	2	228	238	9	1	8	19	143	149	22	2	2	2	1331	1359	6	2	4	11	199	251	11
1	5	3	350	345	13	1	8	20	182	159	18	2	2	3	286	317	11	2	4	12	133	128	16
1	5	4	128	95	14	1	9	3	146	135	21	2	2	4	405	417	10	2	4	13	302	269	13
1	5	7	132	89	14	1	9	10	169	258	19	2	2	5	509	534	9	2	4	14	192	179	13
1	5	8	140	140	14	1	9	18	174	192	19	2	2	6	534	526	9	2	4	15	157	147	15
1	5	10	163	171	13	1	11	3	155	69	20	2	2	7	106	149	15	2	4	16	421	397	15
1	5	12	279	266	11	2	0	0	264	262	8	2	2	8	947	941	8	2	4	17	133	172	19
1	5	13	223	170	11	2	0	1	450	428	6	2	2	9	333	313	11	2	4	18	221	217	13
1	5	14	267	246	12	2	0	2	1057	1074	5	2	2	10	260	333	12	2	4	20	168	172	17
1	5	16	205	210	13	2	0	3	601	608	6	2	2	11	334	309	12	2	4	21	205	248	15
1	5	18	219	207	14	2	0	4	173	194	9	2	2	12	440	477	11	2	4	24	180	164	17

H	K	L	Fobs	Fcalc	SigF	H	K	L	Fobs	Fcalc	SigF	H	K	L	Fobs	Fcalc	SigF	H	K	L	Fobs	Fcalc	SigF
2	5	0	268	246	9	2	9	0	244	178	14	3	1	30	148	85	21	3	4	0	182	104	10
2	5	1	128	141	15	2	9	6	173	164	18	3	2	0	824	793	8	3	4	1	214	194	12
2	5	2	444	441	12	2	9	12	164	172	19	3	2	1	172	121	10	3	4	2	565	538	10
2	5	3	767	762	9	2	9	14	249	208	14	3	2	2	195	254	9	3	4	3	437	460	11
2	5	4	118	113	16	2	10	1	224	195	15	3	2	3	101	73	15	3	4	4	161	170	12
2	5	5	672	671	10	2	10	13	150	107	21	3	2	4	251	301	9	3	4	5	126	154	14
2	5	6	622	554	10	3	0	1	198	82	8	3	2	5	121	141	13	3	4	6	349	333	14
2	5	9	409	459	14	3	0	3	312	340	12	3	2	6	409	362	10	3	4	7	195	225	11
2	5	10	178	148	13	3	0	4	1261	1182	7	3	2	7	140	176	12	3	4	8	262	303	12
2	5	11	246	210	10	3	0	5	313	334	12	3	2	8	426	439	11	3	4	9	179	174	11
2	5	13	133	143	18	3	0	6	117	191	13	3	2	9	304	300	11	3	4	10	681	686	11
2	5	15	138	144	18	3	0	7	149	291	10	3	2	10	128	119	14	3	4	11	385	370	14
2	5	17	381	380	13	3	0	9	289	224	11	3	2	11	138	101	13	3	4	12	121	127	18
2	5	18	305	287	14	3	0	10	239	253	12	3	2	12	650	669	11	3	4	13	125	134	18
2	5	19	172	159	17	3	0	11	288	351	10	3	2	13	163	133	13	3	4	14	303	298	14
2	5	20	153	83	19	3	0	12	412	469	13	3	2	15	281	256	11	3	4	16	290	336	10
2	5	25	224	238	15	3	0	13	139	119	13	3	2	16	169	112	14	3	4	18	203	252	15
2	6	3	228	211	10	3	0	14	166	116	12	3	2	17	327	317	16	3	4	19	173	178	17
2	6	4	180	218	13	3	0	15	396	331	14	3	2	18	333	315	13	3	4	20	142	127	20
2	6	5	405	390	14	3	0	16	260	282	10	3	2	19	133	79	19	3	5	0	430	492	13
2	6	6	614	583	11	3	0	17	128	114	17	3	2	20	140	189	19	3	5	1	567	615	11
2	6	8	227	173	11	3	0	18	150	250	17	3	2	22	167	133	18	3	5	2	635	689	10
2	6	11	146	181	17	3	0	19	230	235	12	3	2	26	208	181	15	3	5	5	485	466	12
2	6	12	160	161	16	3	0	21	167	166	17	3	3	0	185	162	9	3	5	6	484	505	12
2	6	13	159	176	16	3	1	0	905	879	7	3	3	1	787	753	8	3	5	8	328	286	12
2	6	14	212	203	13	3	1	1	940	893	7	3	3	2	418	392	11	3	5	14	185	161	14
2	6	16	222	208	14	3	1	3	537	491	9	3	3	3	176	175	9	3	5	15	137	159	19
2	6	17	191	150	15	3	1	4	597	626	8	3	3	4	176	166	11	3	5	20	225	166	14
2	6	19	152	111	19	3	1	5	1110	1066	7	3	3	5	136	192	13	3	5	23	272	235	12
2	6	20	214	200	15	3	1	6	794	790	8	3	3	6	423	374	11	3	6	1	280	263	10
2	6	23	155	199	20	3	1	7	860	860	8	3	3	7	329	363	12	3	6	4	315	306	11
2	7	1	146	142	17	3	1	8	392	381	11	3	3	8	402	362	12	3	6	5	139	119	17
2	7	3	182	181	15	3	1	9	265	298	11	3	3	9	137	129	13	3	6	7	172	192	14
2	7	4	417	388	15	3	1	10	281	252	9	3	3	10	328	337	13	3	6	8	325	268	12
2	7	5	259	296	11	3	1	11	233	250	9	3	3	11	333	293	13	3	6	9	248	310	11
2	7	8	258	278	11	3	1	13	316	327	13	3	3	13	389	307	13	3	6	11	273	242	11
2	7	10	187	240	16	3	1	14	282	301	11	3	3	14	315	312	11	3	6	12	314	302	13
2	7	12	242	237	12	3	1	15	571	621	12	3	3	15	239	282	12	3	6	15	142	129	20
2	7	13	202	190	15	3	1	16	140	184	16	3	3	16	327	358	12	3	6	17	143	160	20
2	7	15	158	161	19	3	1	17	299	272	12	3	3	17	389	415	14	3	6	19	165	177	18
2	7	16	258	244	13	3	1	18	171	210	15	3	3	20	156	182	18	3	6	20	142	138	21
2	8	2	173	167	17	3	1	19	163	192	16	3	3	21	298	294	11	3	7	1	282	272	11
2	8	3	324	325	12	3	1	20	195	171	14	3	3	24	142	142	20	3	7	2	168	164	16
2	8	11	207	163	15	3	1	23	275	290	13	3	3	25	167	183	18	3	7	4	157	143	17

Values of 10*Fobs and 10*Fcalc

H	K	L	Fobs	Fcalc	SigF	H	K	L	Fobs	Fcalc	SigF	H	K	L	Fobs	Fcalc	SigF	H	K	L	Fobs	Fcalc	SigF
3	7	9	169	178	18	4	1	17	233	261	12	4	4	13	147	159	17	5	0	2	499	456	11
3	7	10	341	360	13	4	1	19	213	242	14	4	4	14	265	255	11	5	0	6	130	495	14
3	7	18	246	237	14	4	1	22	152	75	19	4	4	16	166	175	17	5	0	11	161	169	13
3	8	1	265	266	12	4	2	1	441	411	11	4	4	18	222	213	14	5	0	18	465	449	16
3	8	2	215	211	15	4	2	2	508	491	10	4	4	20	202	163	15	5	1	0	128	98	14
3	8	3	276	282	12	4	2	3	237	246	10	4	4	21	138	165	21	5	1	1	344	400	12
3	8	5	223	210	14	4	2	4	183	189	10	4	4	23	253	273	13	5	1	2	302	305	10
3	8	10	140	182	21	4	2	6	339	323	13	4	4	24	139	107	21	5	1	3	352	369	13
3	8	12	137	72	21	4	2	8	291	300	15	4	5	0	184	152	13	5	1	4	351	314	13
3	8	13	187	193	16	4	2	9	238	268	9	4	5	1	618	591	11	5	1	5	191	192	11
3	8	17	164	158	18	4	2	10	577	601	11	4	5	3	398	409	15	5	1	7	204	282	12
3	9	6	204	146	16	4	2	11	308	302	15	4	5	4	355	346	15	5	1	8	237	281	9
3	9	8	168	211	19	4	2	13	296	287	12	4	5	5	333	310	13	5	1	9	238	227	9
3	10	1	170	130	18	4	2	16	283	282	12	4	5	6	239	224	11	5	1	10	240	227	10
3	10	5	151	149	21	4	2	17	153	139	16	4	5	7	475	431	13	5	1	12	160	184	15
3	10	7	219	216	16	4	2	18	242	281	12	4	5	10	204	208	13	5	1	13	339	355	15
3	11	8	150	160	21	4	2	21	247	228	13	4	5	12	221	243	13	5	1	14	144	147	16
4	0	0	935	913	8	4	2	24	209	181	14	4	5	15	197	197	15	5	1	15	162	139	15
4	0	1	550	506	9	4	3	0	197	165	11	4	5	16	154	124	19	5	1	16	175	226	15
4	0	2	258	272	11	4	3	1	187	167	11	4	5	18	145	133	20	5	1	17	205	224	14
4	0	3	415	368	10	4	3	2	281	258	12	4	5	19	208	213	15	5	1	18	137	196	20
4	0	9	194	219	10	4	3	3	703	705	10	4	6	0	226	182	11	5	1	21	150	169	19
4	0	10	110	74	15	4	3	4	115	144	15	4	6	1	292	257	13	5	2	2	487	471	11
4	0	11	247	256	11	4	3	5	423	448	12	4	6	2	186	148	14	5	2	4	658	609	10
4	0	12	137	150	14	4	3	6	116	134	16	4	6	3	272	274	10	5	2	5	134	132	15
4	0	14	253	234	12	4	3	9	424	450	13	4	6	8	334	330	12	5	2	7	157	163	13
4	0	15	260	299	11	4	3	10	294	269	13	4	6	15	207	216	15	5	2	8	213	210	11
4	0	19	138	119	18	4	3	11	422	350	13	4	6	16	263	268	13	5	2	9	186	149	12
4	0	20	218	224	14	4	3	12	134	79	16	4	6	17	152	151	19	5	2	10	314	303	12
4	0	22	229	211	13	4	3	15	140	120	18	4	6	19	140	129	20	5	2	12	157	139	15
4	0	23	172	154	17	4	3	17	431	430	17	4	7	0	283	268	12	5	2	14	163	144	15
4	0	26	162	167	18	4	3	21	186	163	15	4	7	2	184	220	15	5	2	16	312	314	10
4	0	28	156	168	20	4	3	25	167	193	18	4	7	3	224	257	13	5	2	17	186	135	15
4	1	1	526	520	9	4	4	0	467	529	12	4	7	4	159	96	17	5	3	0	373	447	13
4	1	2	315	363	12	4	4	1	703	849	10	4	7	5	275	260	13	5	3	1	334	342	13
4	1	3	713	764	9	4	4	2	324	344	11	4	7	6	205	229	15	5	3	2	397	422	14
4	1	7	261	256	11	4	4	3	230	153	10	4	7	12	283	275	12	5	3	3	308	279	13
4	1	8	164	168	11	4	4	4	232	192	9	4	7	13	165	168	19	5	3	4	191	178	12
4	1	9	400	421	12	4	4	5	868	875	10	4	7	14	244	242	13	5	3	5	346	290	11
4	1	10	131	118	14	4	4	6	741	701	10	4	8	5	232	200	14	5	3	6	523	548	12
4	1	11	762	818	10	4	4	7	123	98	17	4	8	7	180	172	17	5	3	7	275	262	12
4	1	13	238	257	10	4	4	8	378	367	13	4	9	5	143	76	20	5	3	8	301	277	12
4	1	14	219	241	12	4	4	10	202	179	12	4	9	8	156	146	20	5	3	11	159	173	16
4	1	15	289	279	11	4	4	12	243	256	11	4	9	10	175	174	19	5	3	12	165	167	15

H	K	L	Fobs	Fcalc	SigF	H	K	L	Fobs	Fcalc	SigF	H	K	L	Fobs	Fcalc	SigF	H	K	L	Fobs	Fcalc	SigF
5	3	14	200	227	14	5	8	7	226	153	14	6	4	14	190	147	15	7	5	1	201	219	16
5	3	18	177	127	16	5	8	8	155	165	20	6	4	15	190	172	16	7	5	3	187	149	17
5	3	20	197	174	15	5	8	9	184	227	17	6	4	16	206	202	14	7	5	6	185	193	16
5	3	23	230	199	14	6	0	0	250	216	10	6	5	4	157	193	17	7	5	7	175	205	17
5	4	2	239	268	10	6	0	1	203	205	14	6	5	9	233	242	13	7	5	8	178	204	18
5	4	3	199	158	12	6	0	3	116	119	17	6	5	13	237	204	14	7	5	12	147	137	21
5	4	4	177	186	13	6	0	12	229	236	12	6	6	2	178	169	17	7	6	8	145	147	20
5	4	6	253	243	10	6	0	16	245	245	12	6	6	4	141	89	20	7	7	2	180	152	18
5	4	8	195	197	13	6	0	18	204	197	15	6	6	5	382	346	11	7	7	7	160	182	20
5	4	12	195	173	14	6	0	24	242	214	13	6	6	7	201	190	15	7	7	10	178	145	17
5	4	13	130	105	20	6	1	0	128	168	16	6	7	1	154	191	20	8	0	18	185	204	16
5	4	14	167	165	17	6	1	1	430	413	14	6	7	4	153	159	20	8	1	0	272	250	12
5	4	17	172	153	17	6	1	2	182	192	12	6	7	7	175	159	18	8	1	1	257	236	12
5	4	23	148	127	20	6	1	3	386	410	13	6	8	0	202	182	16	8	1	2	193	152	15
5	5	1	310	336	16	6	1	9	388	444	15	6	8	6	145	96	19	8	1	3	171	161	17
5	5	2	404	348	15	6	1	11	513	542	14	6	9	0	148	104	22	8	1	13	170	181	17
5	5	3	130	118	19	6	1	13	242	218	11	7	0	4	403	380	14	8	2	8	134	212	21
5	5	6	147	122	17	6	1	15	135	118	19	7	0	5	124	257	19	8	3	1	140	121	21
5	5	7	160	176	16	6	1	17	252	239	12	7	0	11	152	171	17	8	3	10	180	159	16
5	5	8	163	168	17	6	2	1	156	131	15	7	0	13	158	184	18	8	4	4	161	128	19
5	5	9	166	207	16	6	2	2	178	182	13	7	0	15	224	264	13	8	4	5	183	145	17
5	5	10	359	385	13	6	2	3	375	334	12	7	0	16	177	188	16	8	4	8	192	197	16
5	5	11	144	198	19	6	2	4	327	349	12	7	1	0	154	191	16	8	6	1	141	100	21
5	5	13	164	116	17	6	2	5	383	373	14	7	1	3	159	208	16	8	8	5	149	125	21
5	5	16	268	284	12	6	2	6	259	267	12	7	1	5	126	109	19	9	0	14	195	195	16
5	5	18	147	157	20	6	2	7	184	189	13	7	1	18	149	122	19	9	1	1	158	179	19
5	5	20	199	227	15	6	2	8	125	172	19	7	2	2	297	287	11	9	2	4	146	148	20
5	6	2	221	225	13	6	2	9	161	146	15	7	2	6	316	278	12	9	2	6	141	88	20
5	6	3	213	229	13	6	2	11	124	111	19	7	2	9	146	92	18	10	4	6	146	125	22
5	6	4	253	283	11	6	2	14	196	178	15	7	2	14	142	172	20						
5	6	5	212	175	14	6	2	18	170	189	17	7	2	17	174	208	17						
5	6	7	213	197	14	6	2	22	149	218	20	7	3	0	160	147	17						
5	6	8	162	166	18	6	3	0	256	175	10	7	3	1	190	199	14						
5	6	12	162	108	18	6	3	1	308	292	12	7	3	2	193	161	15						
5	6	13	169	174	18	6	3	6	153	155	16	7	3	10	183	156	16						
5	6	14	212	164	14	6	3	7	266	271	11	7	3	16	165	160	17						
5	6	20	141	103	21	6	3	10	193	217	14	7	4	2	173	164	17						
5	7	0	447	500	17	6	3	11	178	188	15	7	4	4	151	135	19						
5	7	1	184	155	16	6	3	13	275	276	11	7	4	6	185	180	16						
5	7	8	184	205	17	6	4	1	337	315	13	7	4	8	231	205	14						
5	7	9	221	219	14	6	4	2	247	230	11	7	4	9	151	83	19						
5	8	1	142	123	21	6	4	6	126	68	19	7	4	12	148	137	19						
5	8	2	175	216	18	6	4	7	190	166	14	7	4	16	164	128	18						
5	8	5	208	189	16	6	4	8	203	232	14	7	5	0	359	421	12						

☆U.S.Government Printing Office: 1989 — 648-056/04138